Irradiating of ATLAS SCT Modules and Detectors in 2002

P. Dervan[k], L. Andricek[h], P. Booth[k], C. Buttar[k], J Carter[b], M. Donega[d], M. D'Onofrio,[d] L. Eklund[m], B. Gallop[a,j], C. Grigson[k], J. Grosse-Knetter[c], M. Mangin-Brinet[d], M. Mikuz[e], J. Pater[g], D. Robinson[b], F. Rosenbaum[l], S. Shimma[f], R. Wallny[c], T. Weidberg[i]

[a] *Dept. of physics and Astronomy, University of Birmingham, UK*
[b] *Cavendish Laboratory, University of Cambridge, UK*
[c] *CERN, CH-1211 Geneva 23, Switzerland*
[d] *University of Geneva, Geneva, Switzerland*
[e] *Jozef Stefan Insitute, Dept. F9, Jamova, SI-1111 Ljubljana, Slovenia*
[f] *KEK, 1-1 Oho, Tsukuba, Ibaraki 305, Japan*
[g] *Dept. of Physics and Astronomy, University of Manchester, Manchester, M13 3PL, UK*
[h] *Max Planck Institut fur Physik, Munich, Germany*
[i] *Oxford University, Keble Road, Oxford OX1 3RH, UK*
[j] *Rutherford Appleton Laboratory, Chilton, Didcot, Oxon, OX11 0QX, UK*
[k] *Dept. of Physics and Astronomy, University of Sheffield, Sheffield, S3 7RH, UK*
[l] *Santa Cruz Institute for Particle Physics, Santa Cruz, CA 95064, USA*
[m] *Dept of Radiation Sciences, Uppsala University, S-751 21, Sweden*

Abstract

This note reports on the irradiation of ATLAS Semiconductor Tracker (SCT) modules and detectors carried out at the ATLAS irradiation facility at the CERN PS T7 area during the year 2002. In total, 15 modules were irradiated, 9 K5 forward modules (which includes 2 K5.1 forward modules), 6 barrel modules, 2 hybrids (one each for the forward and barrel), plus 52 detectors and 6 minis, as well as various other passive components. The different types of dosimetry are described for each irradiation period.

1 Introduction

The silicon strip detectors that will be used in the SCT will operate in radiation levels significantly greater than those in current experiments. The high-radiation levels arise primarily from the large number of minimum bias interactions that occur during each beam crossing. The radiation damage is therefore dominated by low momentum pions, and other hadrons from these interactions. In addition, there are a relatively small number of neutrons resulting from the leakage of hadronic showers in the calorimeter back into the central tracking region. FLUKA [1,2] has been used to simulate the radiation levels. The maximum radiation levels are found in the inner barrel layer and the inner radii of the first forward disk, corresponding to 1.4×10^{14} 1 MeV equivalent neutrons cm^{-2} over 10 years of ATLAS operation [3]. As the radiation levels are only known to within 50%, the maximum design value is taken as 2.1×10^{14} 1 MeV equivalent neutrons cm^{-2}. Using a damage factor of 0.69 for 24 GeV/c protons [3] (beam delivered from the PS, See Section 2) this corresponds to a fluence of 3×10^{14} protons cm^{-2}. New studies have been done [4], but to keep everything consistent the older figures have been used. This level of radiation causes considerable damage to silicon detectors, both in bulk silicon and in the dielectric layer, and to the readout electronics. To ensure that the SCT detectors and modules could survive that level of radiation an irradiation facility was set up at the CERN PS in 1996.

2 Irradiation of detectors and modules

To enable a large number of detectors and modules to be irradiated a dedicated irradiation facility has been established in the East Experimental Hall of the CERN Proton Synchrotron (PS) [5, 6]. The primary beam is used to irradiate the detectors with 24 GeV protons, which are incident on the detectors in approximately 400 ms spills, each containing between 20 and 40 $\times 10^{10}$ protons. Between 1-3 spills are received per 16 second PS super-cycle and the beam spot size is approximately 2 cm $\times$ 2 cm. Because the detectors have a larger area than the beam it is necessary to scan them through it to achieve a uniform irradiation, thus reducing the effective intensity of

the beam and increasing the irradiation times. The target fluence for proton irradiation is 3×10^{14} protons cm^{-2}. This fluence can be achieved in between 9 and 14 days depending on beam conditions. The received fluence is measured using a secondary emission monitor upstream of the irradiation facility calibrated by the activation of aluminium foils [7]. Other forms of dosimetry used in the irradiation are described in Section. 4.

During irradiation, the detectors and modules are kept in a constant environment held at or below the ATLAS SCT designed operating temperature of -7°C. This was achieved by containing the detectors and modules in a thermally insulated Styrofoam enclosure cooled by the passage of an antifreeze-water coolant mixture through heat exchangers. A uniform temperature and a dry atmosphere are maintained through the use of flat pack blower fans and a constant flow of dry nitrogen. Temperatures within the enclosure are monitored at several positions using PT100 thermistors. The thermal enclosure is situated on an x-y stage which is used to scan the detectors through the beam, with a motion program that ensures that the detectors receive a uniform fluence across their whole area. Each detector is biased independently with the strip metal and underlying implanted strips connected to ground and the backplane held at 100 V. The guard rings are floating. Detector currents are monitored and recorded automatically with a current measurement for each detector being taken every 1-3 min for the duration of the irradiation. The modules are also biased to 100 V and the front-end chips, ABCDs [8], are powered and clocked. If time permitted the modules were characterised every 0.5×10^{14} protons cm^{-2} to optimise the front-end setting.

3 Radiation damage in silicon detectors

Irradiation of silicon detectors by charged particles results in damage in the bulk silicon and the dielectric layer [9, 10]. The following describes a method developed in [11]. Damage in the bulk results in two effects: increase in the leakage current of the detector and a change in the effective doping concentration. The latter results in type inversion and affects the depletion voltage. The change in effective doping concentration, N_{eff}, is parameterised

by:

$$N_{eff}(\phi) = N_{eff}(0)e^{-c\phi} - \beta\phi \tag{1}$$

The first term describes the removal of donors and the second term the creation of acceptors: $N_{eff}(0)$ is the initial effective carrier density, c is the rate of donor removal and β is the rate of acceptor creation.

The increase in leakage current, I, is parameterised by:

$$I = \alpha\phi V \tag{2}$$

where I is the current, α is the current damage factor, ϕ is the fluence and V is the detector volume.

To predict the leakage current using the bulk radiation damage parameterisations it is necessary to combine the effects of both the change in effective carrier density and the increase in the leakage current. This is best done by considering the low fluence and high fluence regions separately. The pre-irradiation full depletion voltage for a $300\mu m$ thick detector is typically 60 to 80 V. The detectors are held at a constant bias of 100 V and are thus fully depleted when the irradiation begins. The donor removal term in Eq. 1 initially causes the effective carrier density, and hence the full depletion voltage, to decrease and the detector remains fully depleted with a constant volume. Therefore Eq. 2 implies that a linear relationship between detector current and fluence should be observed at low fluences (assuming the initial detector current to be negligible; initial currents of $I_0 = 0.5\ \mu A$ are observed). Therefore at low fluences we expect:

$$I \propto \phi \tag{3}$$

At high fluences (above approximately 10^{14} protons cm^{-2}) the acceptor creation term in Eq. 1 dominates and to a good approximation $|N_{eff}(\phi)| = \beta\phi$. This results in a full depletion voltage greater than the applied bias voltage,

the detector is no longer depleted and the active volume of the detector is now a function of fluence:

$$V = Aw = A\sqrt{\frac{2\epsilon}{e}\frac{V_{bias}}{|N_{eff}|}} = A\sqrt{\frac{2\epsilon}{e}\frac{V_{bias}}{\beta\phi}} \tag{4}$$

where A is the area of the detector, w is the depletion width of the detector, ϵ is the dielectric constant of silicon, e is the electron charge and V_{bias} is the bias voltage applied to the detector. Thus from Eq. 2 the detector current at high fluence should be given by:

$$I = \alpha A\sqrt{\frac{2\epsilon}{e}\frac{V_{bias}}{\beta}}\phi^{0.5} \tag{5}$$

Therefore at high fluences we expect:

$$I \propto \phi^{0.5} \tag{6}$$

Before the above model can be applied to the detectors, the leakage current measured must be corrected for variations in detector temperature and then normalised to the operating temperature (-10°C for the modules). This is done using the following equation:

$$\left(\frac{I_{Norm}}{I_{Meas}}\right) = \left(\frac{T_{Norm}}{T_{Meas}}\right)^2 exp\left[\frac{E_g}{2k_B}\left(\frac{1}{T_{Meas}} - \frac{1}{T_{Norm}}\right)\right] \tag{7}$$

Where E_g is the effective energy band gap (1.12 eV) and k_b is the Boltzmann's constant. For the detectors the measured temperature is taken to be the ambient temperature in the cool box. The temperature of the detectors in a module are harder to determine as we have the hybrid attached to the detectors. The hybrid temperature and the ambient temperature in the box is recored throughout the run so the following calculation are done to determine the detector temperatures.

3.1 Forward Modules

For the forward modules the thermal resistances are used to calculate the detector temperatures. The thermal resistance of the hybrid, detectors and fan-ins are given by [12]:

$$R_{hyb} = \frac{(T_{hyb} - T_{amb})}{P_{hyb}} \tag{8}$$

$$R_{det} = \frac{(R_{hyb} \times A_{hyb})}{A_{det}} \tag{9}$$

$$R_{fanin} = 110K/W \tag{10}$$

Where T is temperature, R is thermal resistance, A is area, hyb means the hybrid part of the module, det means the detector part, gas means the gas and P is power. The detector temperature is then given by:

$$T_{det} = T_{gas} + (T_{hyb} - T_{gas}) \times \frac{R_{det}}{(R_{det} + R_{fanin})} \tag{11}$$

3.2 Barrel Modules

For barrel modules it is known that the detector is 7°C cooler than the measured hybrid temperature [13].

A method of assuming the damage parameters and working back to determine the fluence is being worked on.

4 Dosimetry

The dosimetry is carried out using the various methods described below.

4.1 Secondary Emission Chamber

Up stream of the irradiation area there is a secondary emission chamber (SEC). This instrument uses the principle of secondary emission of electrons from a metallic plate when charged particles pass through it. The electric charge produced in the SEC is directly proportional to the number of protons, which transverse it. This charge is then collected and then transformed into a digital signal. Approximately 180×10^6 SEC counts is equivalent to 3×10^{14} protons cm^2.

4.2 Aluminium Foils

In most of the irradiations an aluminium foil (99.9% pure) is placed at the back of the irradiation cool box, and is irradiated along with the detector and modules. During the irradiation the aluminium activates and produces radioactive isotopes with know half-lifes [14]:

^{27}Al(p,3pn)^{24}Na
^{27}Al(p,3p3n)^{22}Na
^{27}Al(p,4p6n)^{18}Fe
^{27}Al(p,spall)^{7}Be

The ones of interest in the irradiations are ^{24}Na with a half-life of 14.96 hours, ^{22}Na with a half-life of 2.6 years and ^{7}Be with a half life of 53.29 days. After the irradiation the aluminium foils can be placed in a spectrometer (Germanium detector) that can measure these isotopes accurately (^{22}Na is used for the long ATLAS irradiations and ^{24}Na is used to calibrate the SEC counter). From these numbers and knowing the cross-sections the fluence can be calculated.

4.3 Spectrometry

Whenever any material is irradiated it becomes activated by producing radioactive isotopes (like the Aluminium foils, Section 4.2.), for example the modules or the silicon detectors. The Germanium detector can also be used to measure the activation of these materials, in-order to compare two different irradiations. These comparisons are only relative measurements of the fluence, not absolute ones.

4.4 Detectors Currents

The detector currents in both single detectors and modules should be rising throughout the irradiation as described in Section. 3. The currents in the single detectors are measured every 1 hour automatically and saved onto a log file. At the beginning of the year the module biases were supplied by bench supplies and had to recorded manually into a log book (approximately once every 8 hours). SCTHV cards were not used as they tripped at 5mA. When the beam passes through the detectors the currents can reach 8mA, so the supplies tripped every spill. From the August irradiation onwards current limiters were added so that the SCTHV cards could be used. This meant that the modules detector currents could be readout automatically by the DAQ software, at regular intervals, and stored in a log file. Hence for the first time the currents of both the detectors and the module's detectors could be used as a form of dosimetry. If the detector currents were not increasing with time, they were not receiving the beam. This can be seen in the plots below.

5 2002 Irradiations

The year 2002 had 6 irradiation periods spread throughout the year. Each period is described in detail below.

5.1 Period P1A

This irradiation period began on the 5^{th} May and ran until 16^{th} May. The following modules were irradiated in this period (listed in the order that the beam would have passed through them, cradle 1 upstream of cradle 2):

Cradle 1	Cradle 2
30 Detectors	K5-307 Inner Forward Module Unpowered
6 Mini Detectors	K5-305 Outer Forward Module
B0018 Barrel Hybrid	K5-308 Outer Forward

5.1.1 SEC counter and PS performance

Two spills (one spill was 40×10^{10} protons) per supercycle were delivered day and night throughout the run. The supercycle length was 16.8 seconds. The accumulated fluence (given by the SEC counter) as a function of time is shown in Fig. 1. As can be seen from Fig. 1 the fluence was accumulated at at constant rate throughout the run apart from the first day where no beam was delivered to the East Hall. This was due to problems with a transformer in the septum power supply (the septum extracts the beam from the PS and sends it into the East Hall). In order to run the septum at all the nominal beam energy of 24 GeV had to be reduced to 20 GeV.

5.1.2 Detector Currents

As described in Section. 2 the detectors were kept biased to 100 V and the temperature and detector currents were monitored throughout the run. Using the procedure described in Section. 3 the detector currents were corrected for temperature and the corrected currents for a sample of detectors are shown in Fig. 2. These curves were consistent with ones from previous irradiations [11]. Again dips or level parts can be seen where no beam was delivered on target.

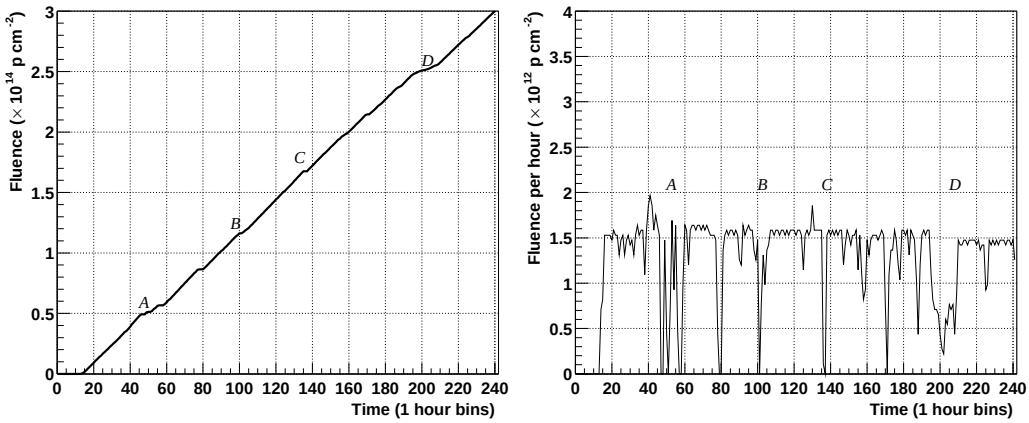

Figure 1: (left) Fluence delivered by the PS as a function of time for the period P1A. The level parts indicate where no beam was delivered on target or the box was out of the beam. (A) Characterisation of the modules and Septum power supply problems. (B) Characterisation of the modules. (C) PS water cooling problems (D) PS timing problems and module characterisation. (right) Fluence delivered per hour.

5.1.3 Module Detector Currents

The module detector currents were also corrected for temperature as described in Section 3. Fig. 3 shows the corrected currents. Note the leakage current for module K5-308 decreased during the run. This was because the detectors for that module started to thermally run away so the detector bias was reduced from 100 V to 60 V.

5.1.4 Foils

The total fluence, as measured from the foils, for this irradiation was:

$$3.3 \times 10^{14} \pm 0.17 \times 10^{14} \text{ protons cm}^{-2}.$$

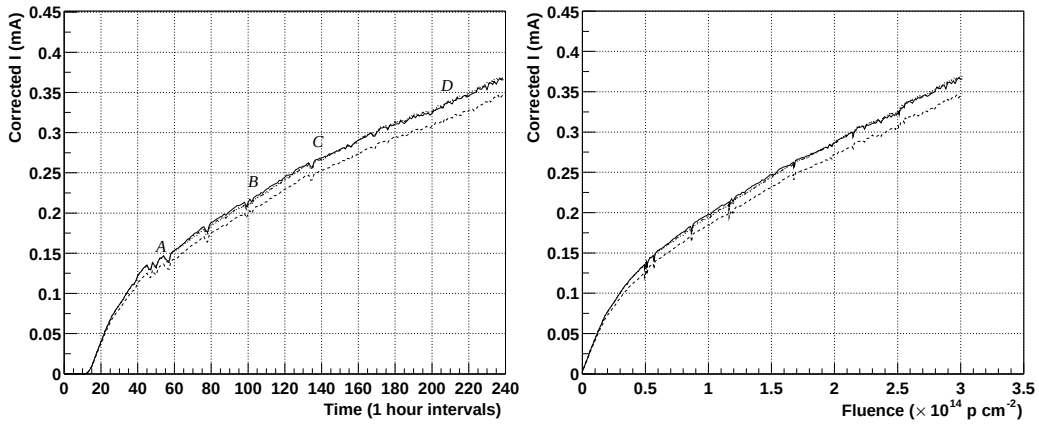

Figure 2: (left) The corrected detector currents, for a sample of those irradiated, as a function of time. The labels are showing times when there was no beam (see Fig. 1) (right) The corrected detector currents as a function of fluence, for period P1A.

3.50 ± 0.56	3.50 ± 0.53	3.43 ± 0.51	3.03 ± 0.52
3.63 ± 0.59	3.76 ± 0.56	3.38 ± 0.30	3.26 ± 0.31
3.28 ± 0.51	3.86 ± 0.58	3.66 ± 0.60	3.26 ± 0.55
3.31 ± 0.31	3.42 ± 0.51	3.21 ± 0.49	2.85 ± 0.48

Table 1: The measured beam profile for period P1A ($\times$ 10^{14} protons cm^{-2})

The foil was then chopped up into equal pieces of approximately 2 cm^2 and re-measured to get the beam profile. Table. 1 shows the measurements of the individual foils and Fig. 4 shows the same information graphically.

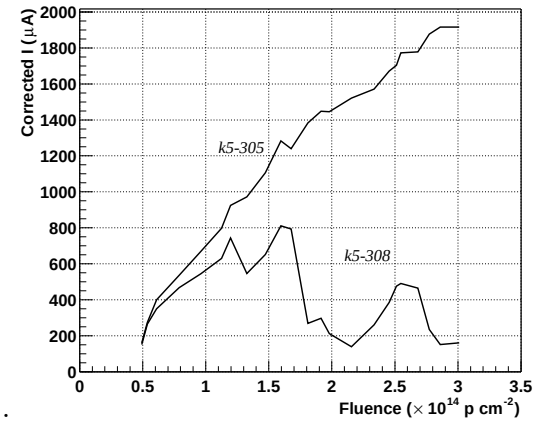

Figure 3: The corrected module detector current as a function of fluence for period P1A.

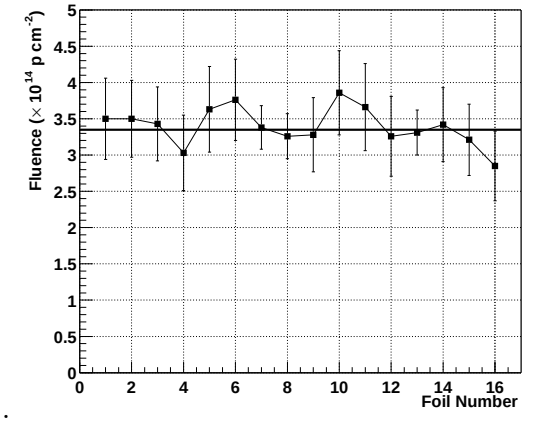

Figure 4: The measured beam profile for period P1A. The line is the mean value.

5.2 Period P1B

This irradiation period began on the 29^{th} May and ran until 12^{th} June. The following modules were irradiated in this period:

Cradle 1	Cradle 2
	B0007 Barrel Module
	B0034 Barrel Module

5.2.1 SEC counter and PS performance

Two spills per supercycle were delivered during the day (8:00-16:00) and one spill per supercycle at night (16:00-8:00) throughout the run. The supercycle was 16.8 seconds long. The accumulated fluence (given by the SEC counter) as a function of time is shown in Fig. 5.

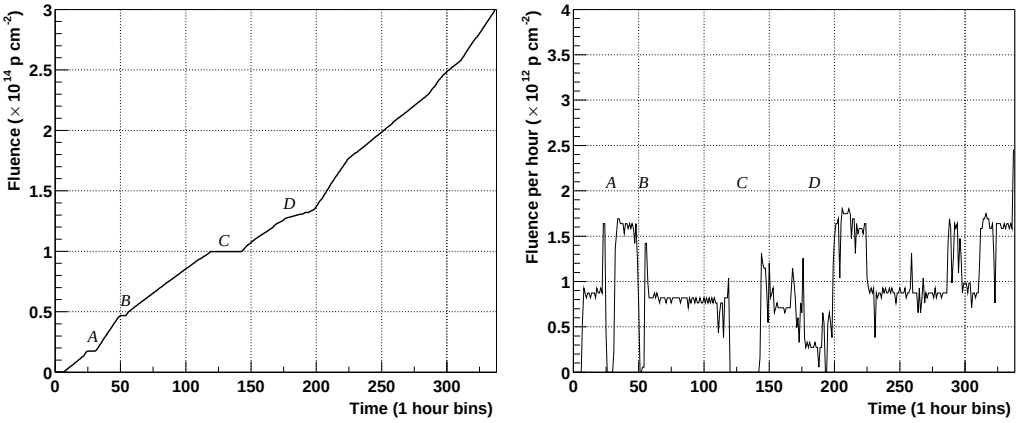

Figure 5: (left) Fluence delivered by the PS as a function of time for the period P1B. (A) Vacuum leak in the Booster. (B) PS cooling water leak, RF cavity fault and module characterisation. (C) Booster vacuum problems. (D) Unstable beam. (right) Fluence delivered per hour.

5.2.2 Module Detector Currents

Fig. 6 shows the corrected currents. The un-even look of the plot is due to the 8 hour gaps between measurements.

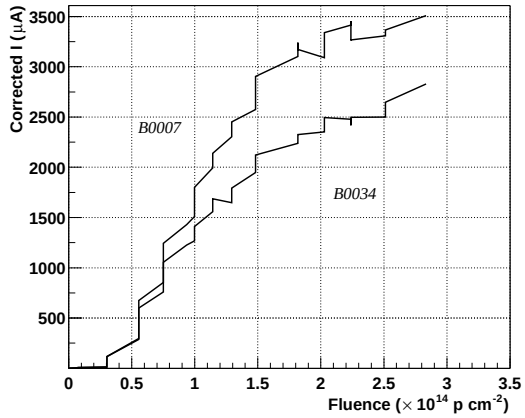

Figure 6: The corrected module detector current as a function of fluence for period P1B.

5.3 Period P1C

This irradiation period began on the 27^{th} June and ran until 9^{th} July. The following modules were irradiated in this period:

Cradle 1	Cradle 2
K5-313 Inner Forward Module Unpowered K5-310 Outer Forward Module K5-312 Outer Forward Module	K5- Forward Module Hybrid

5.3.1 SEC counter and PS performance

Two spills per supercycle were delivered during the day (8:00-16:00) and one spill per supercycle at night (16:00-8:00) throughout the run. The supercycle was 16.8 seconds long. The accumulated fluence (given by the SEC counter) as a function of time is shown in Fig. 7.

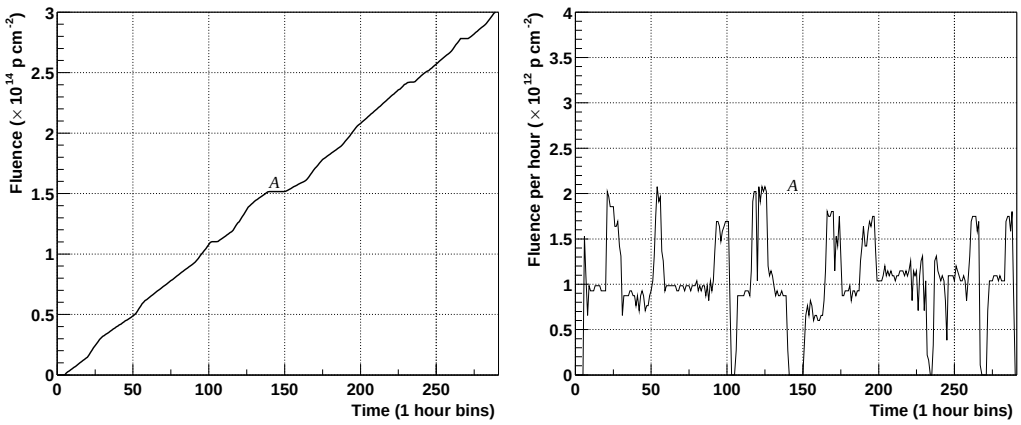

Figure 7: (left) Fluence delivered by the PS as a function of time for the period P1C. (A) PS Machine Development and module characterisation. (right) Fluence delivered per hour.

5.3.2 Module Detector Currents

K5-310 was not biased during this irradiation. The problem was found to be a broken trace on the kapton, that supplied the power and biases to the module.

Fig. 8 shows the corrected currents. Note that no measurements were possible early in the run (up to 1.5×10^{14} protons cm^{-2}) due to SEU (Single Event Upset) measurements being carried out.

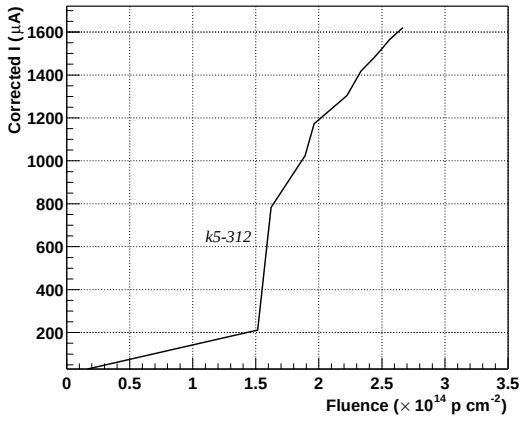

Figure 8: The corrected module detector current as a function of fluence for period P1B.

5.3.3 Spectrometry

There was a big difference in the electrical performance of the modules [15] irradiated in this period and the ones irradiated in period P1A. Unfortunately there was no foil in this irradiation, due to time constraints, so the fluence could not be measured directly. Instead the modules K5-310, K5-312 and K5-308 (K5-305 was in the Rutherford Laboratory for thermal measurements), were measured in the same spectrometer as the foils. A collimator was made

Module	^{22}Na Bq/unit	^{7}Be Bq/unit
K5-308	1.30×10^3	4.60×10^3
K5-310	0.67×10^3	4.10×10^3
K5-312	0.67×10^3	4.40×10^3

Table 2: The activation measurements of K5-308, K5-310 and K5-312.

such that only the activation from a 2 cm^2 area of the far (furthest away from the hybrid) silicon detector was measured. Table 2 shows the results of the activation measurements. This was a relative measurement of the fluence not an absolute measurement.

A factor of two difference in the ^{22}Na activation levels was observed. The half life of ^{7}Be is 53.29 days which is exactly the time difference between the two irradiations. Hence there is also a factor of two from the ^{7}Be. Thus there seems to be a factor of two difference in the received fluence between the two irradiations. Using the ratios an estimated fluence of 1.6×10^{14} protons cm^{-2} was assigned to the modules.

It was decided to irradiate K5-312 with another 1.4×10^{14} protons cm^{-2}. An extra irradiation was applied for and got in period P3A (see Section 5.5).

5.4 Period P2A and P2B

This irradiation period began on the 8^{th} August and ran until 19^{th} August. The following modules were irradiated in this period:

Cradle 1	Cradle 2
USQ3 Barrel Module B0096 Barrel Module	22 detectors

5.4.1 SEC counter and PS performance

The number of spills delivered during this run varied between 1 and 3 spills per supercycle, depending on PS operation. The supercycle length was 16.8 seconds long. The accumulated fluence (given by the SEC counter) as a function of time is shown in Fig. 9.

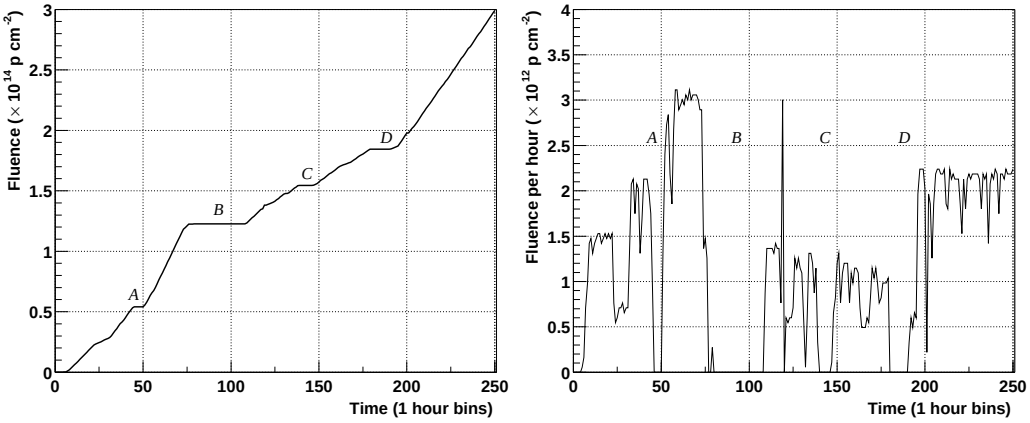

Figure 9: (left) Fluence delivered by the PS as a function of time for the period P2A and P2B. (A) Module characterisation. (B) Septum Magnet 57 broken and lumps are also due to the septum magnet tripping. (C) Module characterisation. (D) Septum magnet problems. (right) Fluence delivered per hour.

5.4.2 Detector Currents

The detector currents were corrected for temperature and the corrected currents for a sample of detectors are shown in Fig. 10. The big bump at 1.2×10^{14} protons cm^{-2} is due to the cool box being thermally cycled.

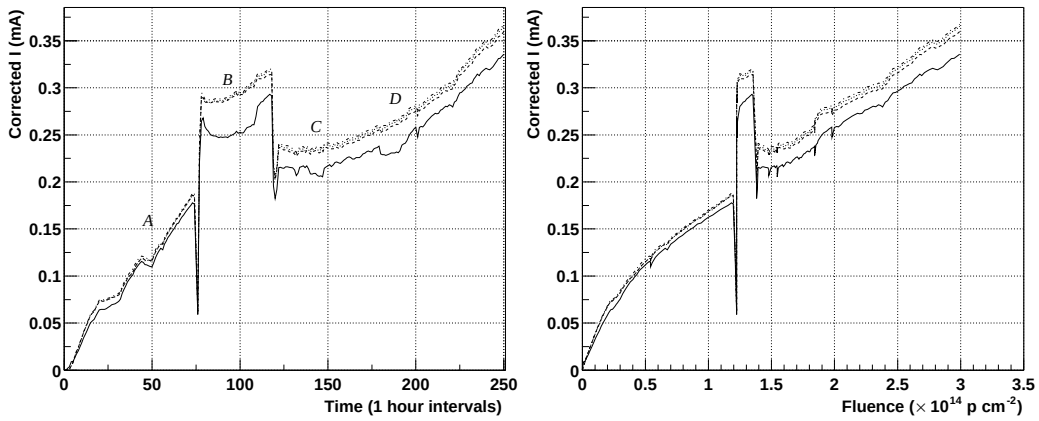

Figure 10: (left) The corrected detector currents, for a sample of those irradiated, as a function of time. The labels are showing times when there was no beam (see Fig. 9) (right) The corrected detector currents as a function of fluence, for period P2A and P2B.

5.4.3 Module Detector Currents

This was the first irradiation where the module detector bias was supplied by a SCTHV card. Enabling the currents to be read out at frequent intervals throughout the irradiation.

Fig. 11 shows the corrected module detector currents as a function of time and as a function of fluence.

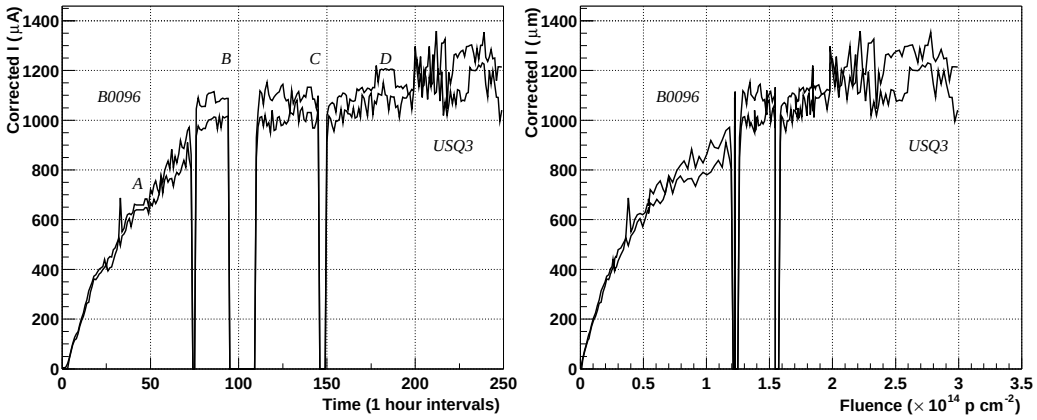

Figure 11: (left) The corrected module detector current as a function of time. The labels are showing times when there was no beam (see Fig. 9) (right) The corrected module detector current as a function of fluence for period P2A and P2B.

5.4.4 Foils

The total fluence, as measured from the foils, for this irradiation was:

$$2.77 \times 10^{14} \pm 0.19 \times 10^{14} \text{ protons cm}^{-2}.$$

The foil was then chopped up into equal pieces of approximately 2 cm^2 and re-measured to get the beam profile. Table. 3 shows the measurements of the individual foils and Fig. 12 shows the same information graphically.

2.73 ± 0.19	2.79 ± 0.29	3.38 ± 0.31
2.79 ± 0.19	2.92 ± 0.25	2.79 ± 0.19
2.72 ± 0.23	2.74 ± 0.23	2.66 ± 0.18

Table 3: The measured beam profile for period P2A and P2B ($\times 10^{14}$ protons cm^{-2})

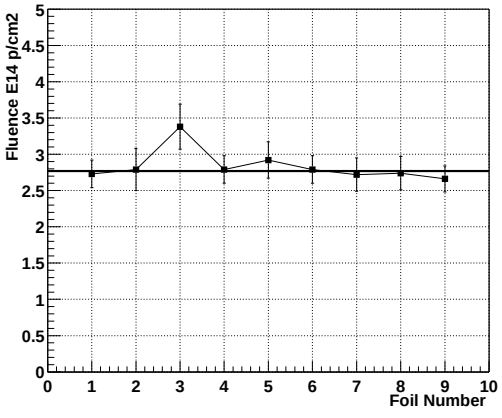

Figure 12: The measured beam profile for period P2A and P2B. The line is the mean value.

5.5 Period P3A

This irradiation period began on the 27^{th} September and ran until 4^{th} October. This was an extra irradiation to get K5-312 up to full fluence. K5-303 was put into the irradiation as a reference. The following modules were irradiated in this period:

Cradle 1	Cradle 2
K5-312 Outer Forward Module K5-303 Outer Forward Module	

5.5.1 SEC counter and PS performance

The number of spills delivered during this run varied between 1 and 2 spills per supercycle, depending on PS operation. The supercycle length was 16.8 seconds long. The accumulated fluence (given by the SEC counter) as a function of time is shown in Fig. 13.

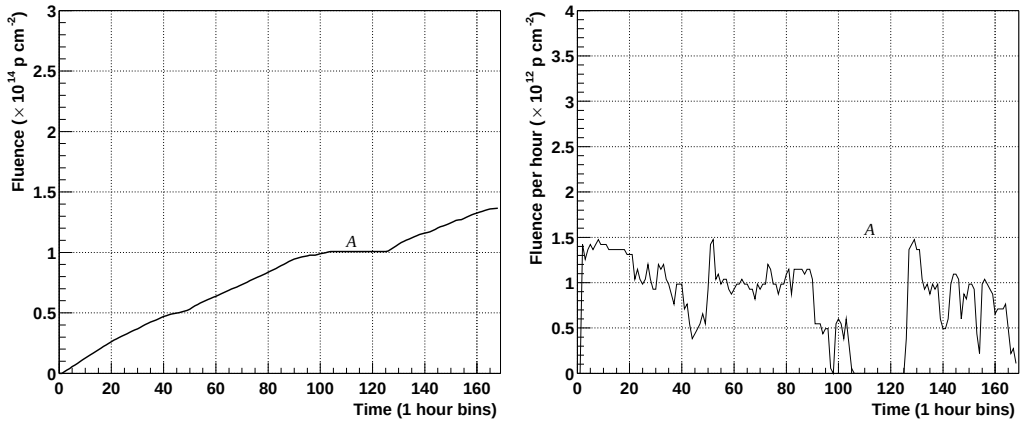

Figure 13: (left) Fluence delivered by the PS as a function of time for the period P3A. (A) Problems with the septum. (right) Fluence delivered per hour.

5.5.2 Module Detector Currents

Fig. 14 shows the corrected module detector currents as a function of time and as a function of fluence. In the fluence plot the 1.6 $\times$ 10^{14} protons cm^{-2} has been added onto the fluence for K5-312, as this module is being irradiated for the second time and 1.6 was the estimated fluence it received in the period P1C.

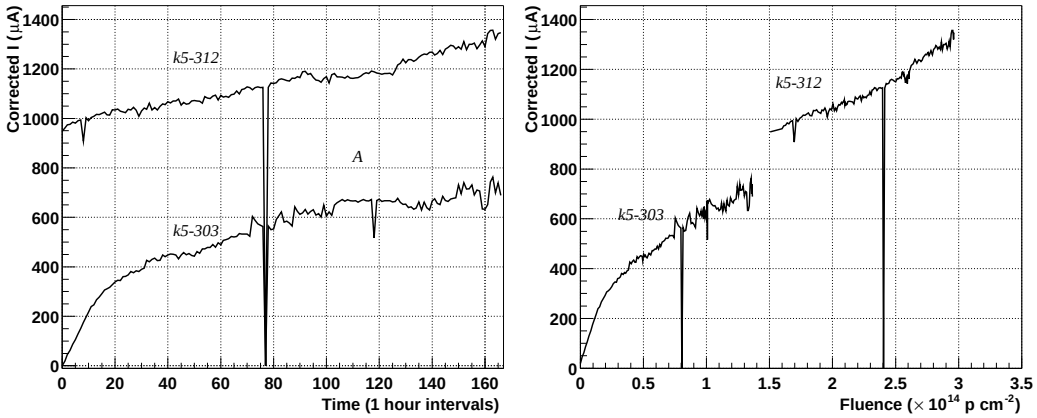

Figure 14: (left) The corrected module detector current as a function of time. The labels are showing times when there was no beam (see Fig. 13) (right) The corrected module detector current as a function of fluence for period P3A.

Dates	Number of Spills per super cycle	Super cycle length (sec)
0ct 18 18:00 - Oct 19 12:00	2	19.2
Oct 19 12:00 - Oct 21 0:00	2	21.6
Oct 21 0:00 - Oct 21 6:00	3	21.6
Oct 21 6:00 - Oct 21 8:00	0	21.6
Oct 21 8:00 - Oct 21 14:00	2	21.6
Oct 21 14:00 - Oct 22 0:00	0	21.6
Oct 22 0:00 - Oct 28 6:00	2	16.8

Table 4: The spill structure and supercycle length for period P3B.

5.6 Period P3B

This irradiation period began on the 17^{th} October and ran until 27^{th} October. The following modules were irradiated in this period:

Cradle 1	Cradle 2
KB-100 Forward Module	B0659 Barrel Module Unpowered
K5-504 Outer Forward Module	B0153 Barrel Module Unpowered
K5-503 Outer Forward Module	

5.6.1 SEC counter and PS performance

The number of spills delivered during this run varied between 1 and 4 spills per supercycle, depending on PS operation. The supercycle length was also altered throughout the run, Table 4, due to the PS and SPS Machine developments (MDs). The accumulated fluence (given by the SEC counter) as a function of time is shown in Fig. 15.

Four spills were delivered for a short time, when DIRAC had technical problems and requested no beam. This can be clearly seen in Fig. 15 at 100 hours.

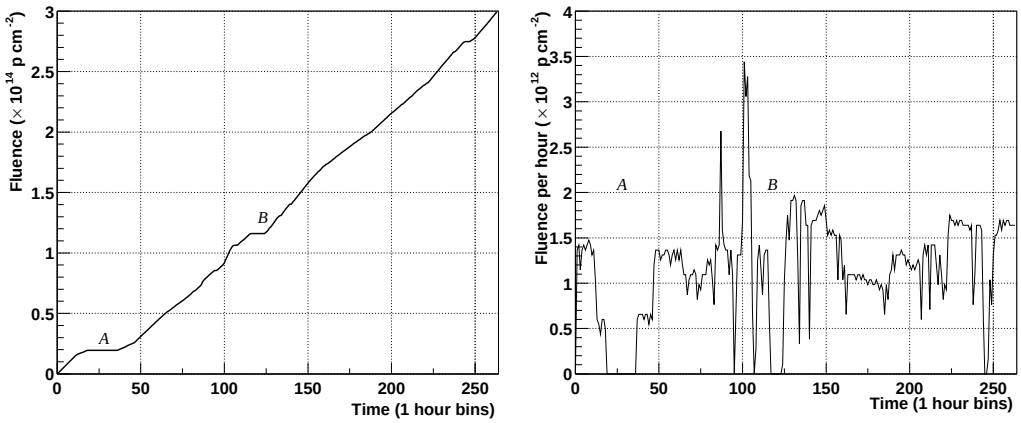

Figure 15: (left) Fluence delivered by the PS as a function of time for the period P3B. (A) Septum power supply flooded (B) Septum problems. (right) Fluence delivered per hour.

5.6.2 Module Detector Currents

The barrel modules were not powered or biased during this run due to problems with connection and the support card in the T7 area.

Fig. 16 shows the corrected module detector currents as a function of time and as a function of fluence. Notice the large difference between the KB module (forward detectors but with a barrel hybrid) and the K5 forward modules. Since the only difference between the two type of modules is the hybrid. This and the consequent difference in the detector temperature must be the difference between the currents. This difference was also seen between the forward and barrel modules (Fig. 19).

5.6.3 Foils

The total fluence, as measured from the foils, for this irradiation was:

$$2.68 \times 10^{14} \pm 0.20 \times 10^{14} \text{ protons cm}^{-2}.$$

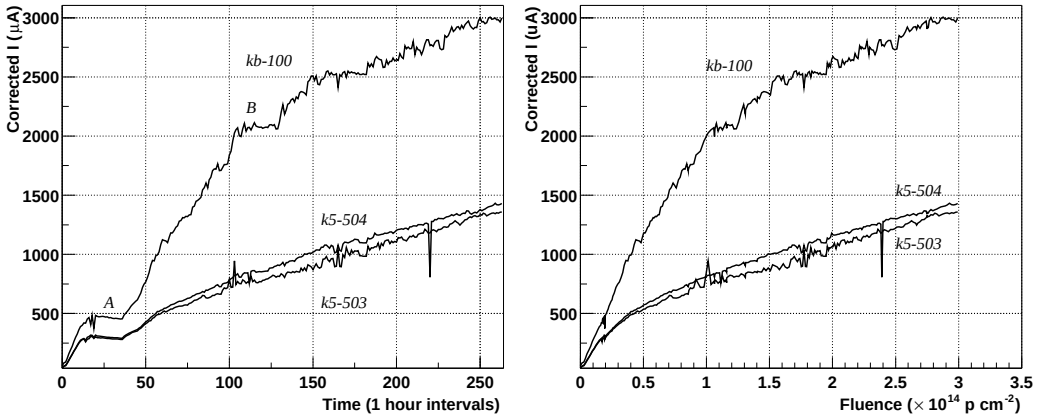

Figure 16: (left) The corrected module detector current as a function of time (the kb-100 is not corrected). The labels are showing times when there was no beam (see Fig. 15) (right) The corrected module detector current as a function of fluence for period P3B.

6 Summary of the 2002 irradiation

Table. 5 lists all the irradiation periods in 2002, along with what was irradiated and in what condition. The fluence for each period measured from foils or from spectrometry is also shown.

Date	Modules	Powered	Biased	Detectors	Foil	fluence*
5^{th} May	K5-305	Y	Y	30	Y	3.3
	K5-308	Y	Y			
	K5-307	N	N			
	B0018 (H)	Y	N			
29^{th} May	B0007	Y	Y		N	
	B0034	Y	Y			
27^{th} June	K5-310	Y	N		N	1.6
	K5-312	Y	Y			
	K5-317	N	N			
	K5-315 (H)	Y	N			
8^{th} August	USQ3	Y	Y	25	Y	2.7
	B0096	Y	Y			
27^{th} September	K5-312	Y	Y	2	Y	
	K5-303	Y	Y			
16^{th} October	K5-503	Y	Y		Y	2.68
	K5-504	Y	Y			
	KB-100	Y	Y			
	B0659	N	N			
	B0153	N	N			

Table 5: The irradiation periods, what was irradiated in them and the fluences received. * The fluence is given in units of $\times 10^{14}$ protons cm^{-2} and (H) denotes a hybrid.

6.1 Dosimetry

6.1.1 SEC counter and PS performance

The PS started running on the 5^{th} May and ran until 28^{th} November, in 2002. The nominal beam energy was reduced to 20 GeV at the start of the run, due to a problem with a transformer in the septum power supply. This septum delivered the beam into the East Hall area. This was the situation until the August run, where it was returned to the normal 24 GeV. Fig. 17 shows the fluence delivered by the PS as a function of time for all the irradiation runs in 2002. As can be see during each of the runs there were periods were no beam was delivered. In each run the PS struggled to reach the required fluence of 3.0×10^{14} protons cm^{-2} in the allocated time (Not indicated).

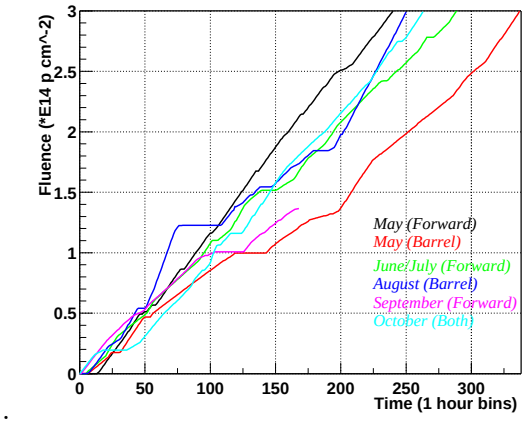

Figure 17: Fluence delivered by the PS as a function of time for each of the irradiation in 2002.

The SEC counter was a reliable indicator of whether beam was being delivered onto target. As can be seen from Figs. 1, 5, 7, 9, 13, 15 any dips in the SEC count verses time were correlated with problems with the PS or the removable of the cool box from the beam for the characterisation of the modules.

6.1.2 Aluminium Foils

Aluminium foils were used to determine the fluence off-line, after the irradiation was over and the modules and detectors removed from the irradiation area. The foils measurements indicate that the SEC counter is correct in calculating the fluence to within 10%.

6.1.3 Spectrometry

Spectrometry was used to investigate the difference between the electrical performance [15] of modules irradiated in Periods P1A and P1C. A factor of ≈ 2 was seen in the activation levels between to two period. This was also backed up by IV measurements after the modules were annealed, Fig 18. The reason for the difference between the two periods is still unknown.

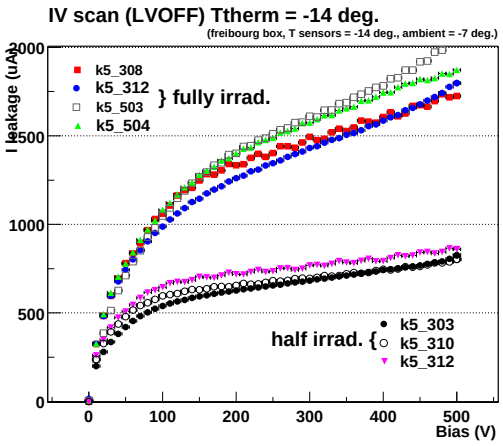

Figure 18: IV curves for forward modules that had half the dose compared to forward modules with full dose, [15]. Which includes K5-312, which was irradiated twice.

6.1.4 Detector Currents

The detector currents could be monitored throughout the run looking for dips in the current verses time plots. Any dips represented no beam on target. This can be seen in Figs. 2 and 10. These dips correlated well with the SEC counter plots. Also the measured currents could be compared to previous irradiations to get an indication of the received fluence.

6.1.5 Module Detector Currents

From Period P2A and P2B, the module detectors were biased from SCTHV cards with current limiters. This meant that the detector currents could be readout and stored at regular intervals throughout the irradiation. Hence the same methods of looking for dips in the currents verses time (Section. 6.1.4) could be used to determine if there was beam on target. So comparing module detector currents with previous irradiations could give us an indication of the received fluence (as with the detector currents). Fig. 19 shows the currents of all the modules since August as a function of fluence.

Note the difference between the barrel (and KB) and the forward modules. This is probably due to the difference in the hybrid or the temperature of the detectors between to two types of hybrid.

7 Summary

Full sized ATLAS silicon microstrip detectors and modules have been irradiated to the predicted 10 year dose using a beam of 24 GeV protons extracted from the CERN PS. The detectors and modules were cooled and held under bias during irradiation and the detector currents were recored throughout. Various methods of dosimetry have been described and used in each of the irradiations to determine the total fluence.

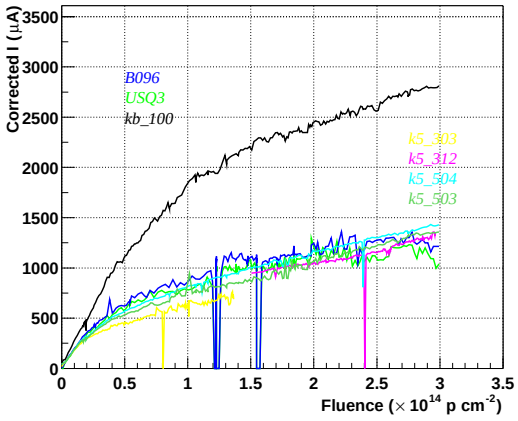

Figure 19: The corrected module detector current (kb-100 is not corrected) as a function of fluence for all modules irradiated since August.

Acknowledgements

The authors would like to thank Michael Hauschild and all the PS staff for their continuous fight to provide the irradiation facility with beam. They would also like to thank M. Glaser and M. Moll from CERN TA1, R. Nicholson and B. Kitchener from the University of Sheffield, Alick McPherson CERN/PSI and all the module building/testing sites; Geneva University, the UK-V forward cluster, the KEK barrel cluster, the UK barrel cluster, the US barrel cluster.

References

[1] A, Fasso, et al., Proceeding of the Third Workshop of Simulating Accelerator Radiation Environments (SARE-3), KEK, Tsukuba, Japan, 1997, p.32.

[2] A. Ferrari, et al., Proceeding of the Third Workshop of Simulating Accelerator Radiation Environments (SARE-3), KEK, Tsukuba, Japan, 1997, p.165.

[3] ATLAS Inner Detector Technical Design Report, CERN/LHCC/97-17, 1997.

[4] I. Dawson, et al., Nucl. Inst. and Meth. A 453 (2000) 461.

[5] D. Morgan, Semiconductor detectors for the inner tracker of the ATLAS experiment at CERN, h.D. Thesis, University of Sheffield, Sheffield, UK (200).

[6] M. Glaser, et al., Nucl. Inst. and Meth. A 426 (1999) 72.

[7] K. Bernier, et al., Calibration of secondary emission monitors of absolute proton beam intensity in the CERN SPS North Area, CERN 97-07, 1997.

[8] SCT Collaboration, ATLAS, ABCD: Project Specification ABCD3T ASIC: V1.2 24 July 2000.

[9] R. Wunstorf, IEEE Trans. Nucl. Sci. NS 44 (1997) 806.

[10] G. Lindstrom, et al., Nucl. Instr. and Meth 426 (1999) 1.

[11] R. S. Harper, et al., Nucl. Instr. and Meth 479 (2002) 548.

[12] S.Snow, Private communication.

[13] Y. Unno, Private communication.

[14] M. Glaser, Private communication.

[15] Draft ATLAS FDR follow-up, Electrical Results from Prototype Modules, http://alpha.ific.uv.es/∼lacasta/ElectricTeam/FDR/